Automatic Pneumonia Screening from X-Ray Image Using Resnet-50 Convolutional Neural Network

Thanagorn Buasomboon, Thaman Toobunterng, Thitapa Thanawasumongkol, Nuntachai Thongpance, Phitsini Suvarnaphaet and Suejit Pechprasarn*

College of Biomedical Engineering, Rangsit University, Pathum Thani, Thailand
*Corresponding author, E-mail: suejit.p@rsu.ac.th

Abstract

Coronavirus disease (COVID-19) is a current global severe health concern that causes a high death risk due to significant alveolar injury and gradual respiratory failure. There are increasing numbers of COVID-19 patients, and they are difficult to be diagnosed and classified. Thanks to one of its primary symptoms, which is Pneumonia, the diagnosis typically involves chest x-ray imaging interpreted by a specialized medical doctor or a radiologist. In this study, artificial intelligence based on Convolutional Neural Network has been developed to identify and classify patients with Pneumonia and assist medical practitioners and doctors in diagnosis as a second opinion. This deep learning software aims for the rapid diagnosis of an X-ray image. Here, the deep learning model was trained with more than 3,000 chest X-ray images with Pneumonia and healthy cases. The Resnet-50 convolutional neural network can successfully perform the classification task of Pneumonia with a classification accuracy of 99.66%.

Keywords**:** *Covid–19, SARS–CoV–2, Pneumonia, Deep learning, Resnet–50, Convolutional neural network, Automated classification*

1. Introduction

An outbreak of a novel coronavirus disease (COVID-19, previously named 2019-nCoV) (Wu, Leung & Leung, 2020) has been firstly reported in Wuhan City, Hubei Province, China, since late December 2019 (Huang, Chaolin, et al., 2020; Qun Li, 2020). The outbreak has been continually evolving, affecting other parts of China and other countries (World Health Organization, 2020). The COVID-19 is a life-threatening disease that causes a high death risk due to significant alveolar injury and gradual respiratory failure (Chan et al., 2020). Coronaviruses (CoV) are a large family of viruses that cause severe lung infection, such as Pandemic influenza (Cooper et al., 2006; Ferguson et al., 2006; Lemey P et al., 2014; Leonid A. Rvachev and Ira M. Longini, 1985), Severe Acute Respiratory Syndrome (SARS) (Hollingsworth and T Déirdre et al., 2006; Hufnagel, L et al., 2004), and Middle East respiratory syndrome coronavirus (MERS- CoV) (Poletto et al., 2014). In 2003, Asia reported the first case of SARS (severe acute respiratory syndrome (Skowronski, Danuta M, et al., 2005)). The total incidence accounted for 8,422 cases of SARS from 29 countries (Centers for Disease Control and Prevention, 2003). Middle Eastern Respiratory Syndrome (MERS) first appeared in 2012 in Saudi Arabia, in which 27 countries were affected worldwide, and 2,494 laboratory-confirmed infection cases have been reported to the World Health Organization (WHO), including 858 related deaths (de Wit, Emmie, et al., 2013). In comparison, the outbreak of the COVID-19 has spread to over 99,864,391 people in 224 countries, accounting for 2,149,700 deaths (Velavan, Thirumalaisamy P, and Christian G Meyer, 2020).

The increasing number of people infected with the COVID-19 causes insufficient medical staff (e.g. doctors, radiologists, and nurses), resulting in delayed treatment of infected patients, which may increase mortality and widespread infection. It is also difficult to pinpoint the viral infection. Two patients with erroneous-positive results from dengue testing in Singapore were later confirmed to have a severe acute COVID-19 (Yan, Gabriel, et al., 2020).

Recently, deep learning approaches can achieve expert-level performance in medical image interpretation tasks (Chapman et al., 2001). There is an observation that through machine learning algorithms, the analysis made can be more precise compared to manual pathologists (Greenspan, van Ginneken and

Summers, 2016). It is explained that most respiratory diseases can be spatially distinguished under chest X-ray imaging and can be identified by supervised multi-label image classification through artificial neural networks and an X-ray image dataset (Shin et al., 2016). It would be an additional preamble to doctors to diagnose these cases precisely to mitigate the problem of misdiagnosis and mitigate the problem of shortage of doctors diagnosing these cases for better and faster providing of treatments to the patients and taking preventive measures more quickly.

2. Objectives

This research aims to study and enhance the accuracy in diagnosing Pneumonia disease from chest X-ray images using a deep convolutional neural network (CNN) with Resnet-50 artificial neural network architecture.

3. Materials and Methods

3.1 Dataset

The chest X-ray images analyzed in this study were downloaded from the NIH Clinical Center database (Xiaosong Wang et al., 2017). It is an open-source database consisting of 112,120 images of 1024x1024 pixel resolution of chest X-ray from 32,717 patients. There are 14 abnormalities, including Atelectasis, Cardiomegaly, Consolidation, Edema, Effusion, Emphysema, Fibrosis, Hernia, Infiltration, Mass, Nodule, Pleural Thickening, Pneumonia, Pneumothorax, and 1 No finding case that is resulted from Chest X-ray. These chest X-ray images are in 8-bit greyscale format. All the training was performed under an Intel(R) Core (TM) i5-9400F @ 2.90 GHz laptop with integrated NVIDIA GeForce GTX1660, Window 10, 16 GB memory. The CNN software was implemented in MATLAB 2019b using the deep learning toolbox.

In this study, the selected images are summarized in Table 1.

Table 1 Distribution of selected images in the dataset

Types	Number of images
Pneumonia	1,500
No Finding	1,500
Total	3,000

3.2 Dataset preparation

Once all the 3,000 selected chest X-ray images were downloaded from the opensource NIH database, all photos were resized to 224 x 224 pixels with three color channels of RGB and sorted with corresponding symptom names. The sorted images were employed as the input dataset for neural network training, and the folder names were used as the corresponding label during the training. The artificial neural network structure details are described in detail in the next section.

3.3 Convolution Neural Network architecture

This paper introduces and assesses the Convolution Neural Network (CNN) architecture's performance in the pre-trained Resnet-50 Model (RCNN) network, and its network architecture is shown in Figure 1 and Table 2 for Pneumonia disease classification. The CNN structure operates and relies on two main types of transformations: convolution, in which pixels in the analyzed image are convolved with a kernel filter. The width and height of the filter can be set to any square matrix size. The usual length of the kernel for the convolutional operator is set to a 3 x 3 matrix. The filter's depth is usually set to the same as the depth of input – secondly, subsampling operators, such as max pooling, min pooling, and average pooling. The user selects the size of pooling, generally be used in odd numbers. The pooling layer is responsible for minimizing the data's size by excluding the image regions containing no information like a blank region or regions that are not the main characteristic features of illnesses.

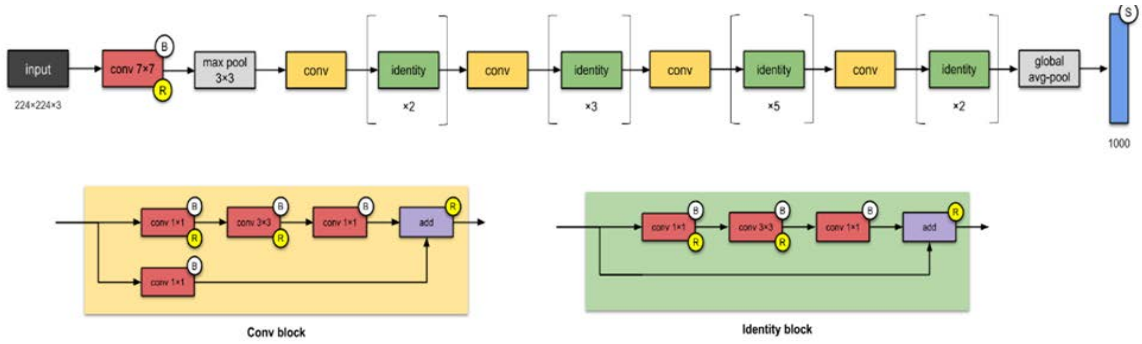

Figure 1 The network architecture shows the Resnet-50 model or RCNN architecture.

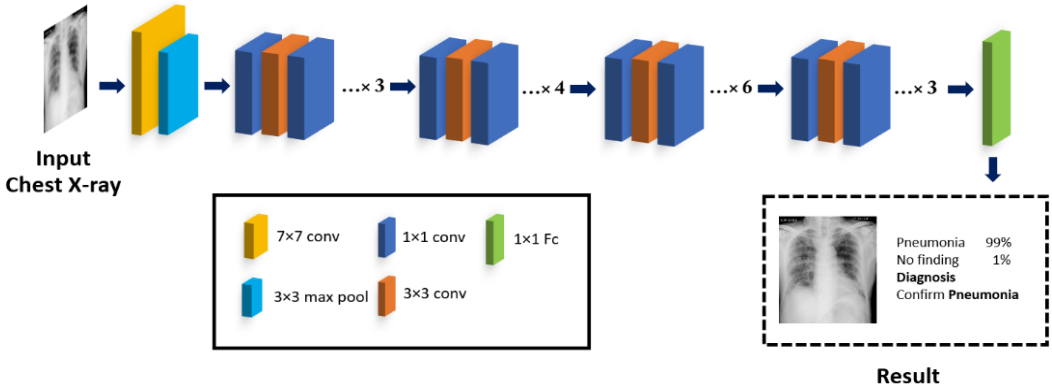

Figure 2 The network architecture with the input and output employed in this study.

Table 2 Parameters of the RCNN architecture (Saining Xie et al., 2017)

Group layer	Output size	Structure	# of group layer
Conv1	112x112	7x7, 64, stride 2	1
Max pooling	112x112	3x3 max pool, stride 2	1
Conv2	56x56	1x1, 64 3x3, 64 1x1, 256	3
Conv3	28x28	1x1, 128 3x3, 128 1x1, 512	4
Conv4	14x14	1x1, 256 3x3, 256 1x1, 1024	6
Conv5	7x7	1x1, 512 3x3, 512 1x1, 2048	3
Classification	1x1	Global average pool 2-d fc, SoftMax, classification	1
# of parameter		$25.5x10^6$	

The RCNN network consists of 177 layers of convolutional filter and pooling layer pair. Here only 2 cases from the dataset were included in this study: Pneumonia and No finding due to their larger database size for training and the urgency needed by the current COVID-19 outbreak. 3,000 images were randomly selected from each group of the two mentioned cases. Each of the folders used all images for training the network. During the training, each image was subdivided into small sub-images with 224 pixels x 224 pixels with three channels of colors and the total minibatch size of 8 sub-images for one x-ray image. Finally, test validation accuracy or overall accuracy with 40 pictures of X-ray images was not included in the training dataset. There were 10 cases of general Pneumonia, 10 cases of COVID-19 Pneumonia, and 20 cases of No finding in the validation set.

4. Results and Discussion

In this study, the authors have employed the RCNN architecture described in the earlier section and trained the RCNN to classify the two types.

Table 3 All test images and their diagnosis comparison between the proposed AI and medical doctor.

Image number [ref]	Figure	Diagnosis by the proposed AI	Diagnosis by a medical doctor
F1 (Chong, KS. et al., 2020)		Pneumonia Confirm 93%	Covid-19 Pneumonia
F2 (Phan, Lan T, et al., 2020)		Pneumonia Confirm 99%	Covid-19 Pneumonia
F3 (Liu, Ying-Chu, et al., 2020)		Pneumonia Confirm 99%	Covid-19 Pneumonia
F4 (Chen, Nanshan, et al., 2020)		Pneumonia Confirm 99%	Covid-19 Pneumonia
F5 (Silverstein, William Kyle, et al., 2020)		Pneumonia Confirm 77%	Covid-19 Pneumonia
F7 (Holshue, Michelle L., et al., 2020)		Pneumonia Confirm 90%	Covid-19 Pneumonia

Image number [ref]	Figure	Diagnosis by the proposed AI	Diagnosis by a medical doctor
F8 (Aljondi, Rowa, and Salem Alghamdi, 2020)		Pneumonia Confirm 99%	Covid-19 Pneumonia
F9 (Aljondi, Rowa, and Salem Alghamdi, 2020)		Pneumonia Confirm 99%	Covid-19 Pneumonia
F10 (Kong, Weifang, and Prachi P. Agarwal)		Pneumonia Confirm 81%	Covid-19 Pneumonia
F11 (Chong, KS. et al., 2020)		Pneumonia Confirm 98%	Pneumonia
F12 (Sheikh, Y., 2020)		Pneumonia Confirm 99%	Pneumonia
F13 (Dixon, A., 2020)		Pneumonia Confirm 99%	Pneumonia
F14 (Khateeb, A., 2020)		Pneumonia Confirm 93%	Pneumonia
F15 (Gaillard, F., 2020)		Pneumonia Confirm 99%	Pneumonia
F16 (Alasaly, K et al., 1995)		Pneumonia Confirm 69%	Pneumonia

Image number [ref]	Figure	Diagnosis by the proposed AI	Diagnosis by a medical doctor
F17 (Heyworth, P., 2020)		Pneumonia Confirm 99%	Pneumonia
F18 (Knipe, H., 2020)		Pneumonia Confirm 99%	Pneumonia
F19 (Knipe, H., 2020)		Pneumonia Confirm 92%	Pneumonia
F20 (Dixon, A., 2020)		No finding Confirm 58%	Pneumonia
F21 (Xiaosong Wang et al., 2017).		No finding Confirm 99%	No finding (Normal)
F22 (Xiaosong Wang et al., 2017).		No finding Confirm 81%	No finding (Normal)
F23 (Xiaosong Wang et al., 2017).		No finding Confirm 93%	No finding (Normal)
F24 (Xiaosong Wang et al., 2017).		No finding Confirm 99%	No finding (Normal)
F25 (Xiaosong Wang et al., 2017).		No finding Confirm 99%	No finding (Normal)

Image number [ref]	Figure	Diagnosis by the proposed AI	Diagnosis by a medical doctor
F26 (Xiaosong Wang et al., 2017).		No finding Confirm 65%	No finding (Normal)
F27 (Xiaosong Wang et al., 2017).		No finding Confirm 98%	No finding (Normal)
F28 (Xiaosong Wang et al., 2017).		No finding Confirm 94%	No finding (Normal)
F29 (Xiaosong Wang et al., 2017).		No finding Confirm 99%	No finding (Normal)
F30 (Xiaosong Wang et al., 2017).		No finding Confirm 99%	No finding (Normal)
F31 (Xiaosong Wang et al., 2017).		No finding Confirm 98%	No finding (Normal)
F32 (Xiaosong Wang et al., 2017).		No finding Confirm 99%	No finding (Normal)
F33 (Xiaosong Wang et al., 2017).		No finding Confirm 99%	No finding (Normal)
F34 (Xiaosong Wang et al., 2017).		No finding Confirm 99%	No finding (Normal)

Image number [ref]	Figure	Diagnosis by the proposed AI	Diagnosis by a medical doctor
F35 (Xiaosong Wang et al., 2017).		No finding Confirm 76%	No finding (Normal)
F36 (Xiaosong Wang et al., 2017).		No finding Confirm 70%	No finding (Normal)
F37 (Xiaosong Wang et al., 2017).		No finding Confirm 95%	No finding (Normal)
F38 (Xiaosong Wang et al., 2017).		No finding Confirm 71%	No finding (Normal)
F39 (Xiaosong Wang et al., 2017).		No finding Confirm 87%	No finding (Normal)
F40 (Xiaosong Wang et al., 2017).		No finding Confirm 79%	No finding (Normal)

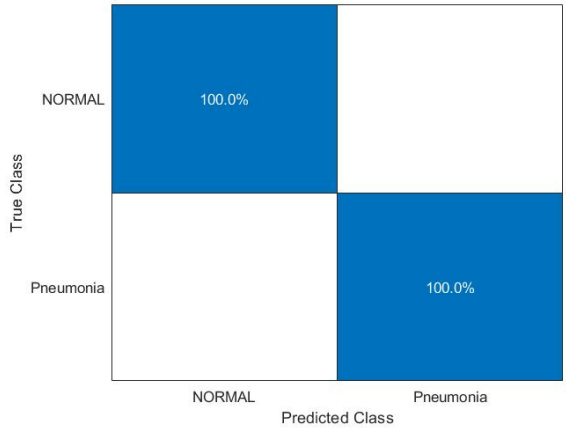

Figure 3 Confusion matrix of the prediction of validation dataset using the RCNN.

The results can be summarized as shown in Figure 3, the overall accuracy is 99.66%, and there were five false-positive images from 40 validation images. On the other hand, this proposed AI has a false positive rate of 0.34%. All the detailed validation results are listed in Table 3. It is important to note that some validation images had similar probabilities on both categories, such as image number F20 with its possibilities of No-finding (normal condition) and Pneumonia (abnormal infection) of 58% and 42%, respectively, which could lead to a false-positive decision of the proposed AI.

This proposed AI (RCNN) can classify between a No-finding case and a Pneumonia case. As the overall accuracy is more than 99%, this proposed AI can serve as a second opinion for medical diagnosis and hopefully as a provisional screen tool to reduce the heavy burden on the medical.

5. Conclusion

This paper has demonstrated that the described CNN architecture and pre-trained network RCNN can be employed to accurately classify x-ray images identifying Pneumonia disease, which is strongly related to the COVID-19. The classification accuracy was 99.66%. Although the trained network has achieved an acceptable accuracy, the number of datasets employed in training was somewhat limited. As the proposed AI (RCNN) was trained with only 3,000 images for the Pneumonia case and the normal case, it still has the false-positive decreasing overall accuracy. In the current state, the authors cannot further classify between conventional Pneumonia and the COVID-19 due to insufficient chest X-ray images from the COVID-19 patients. Therefore, this project's future plan is to increase accuracy, reduce false-positive, and classify the COVID-19 from the conventional Pneumonia by collaborating with hospitals and relevant sections to combat and overcome the harmful virus as soon as possible.

6. Acknowledgements

We would like to express our sincere gratitude the Biophysics & medical optics laboratory of the College of Biomedical Engineering at Rangsit University.

7. References

Wu, J. T., Leung, K., & Leung, G. M. (2020). Nowcasting and forecasting the potential domestic and international spread of the 2019-nCoV outbreak originating in Wuhan, China: a modelling study. The Lancet, 395(10225), 689-697.

Huang, C., Wang, Y., Li, X., Ren, L., Zhao, J., Hu, Y., ... & Cao, B. (2020). Clinical features of patients infected with 2019 novel coronavirus in Wuhan, China. *The lancet*, *395*(10223), 497-506.

Li, Q. (2020). An outbreak of NCIP (2019-nCoV) infection in China—Wuhan, Hubei Province, 2019–2020. China CDC Weekly, 2, 79-80.

World Health Organization. (2020). Novel Coronavirus (COVID-19) Situation Report-44. Retrieved March 4, 2020, from https://www.who.int/docs/default-source/coronaviruse/situation-reports/20200123-sitrep-3-COVID-19.pdf?sfvrsn=d6d23643_4karin

Chan, J. F. W., Yuan, S., Kok, K. H., To, K. K. W., Chu, H., Yang, J., ... & Yuen, K. Y. (2020). A familial cluster of pneumonia associated with the 2019 novel coronavirus indicating person-to-person transmission: a study of a family cluster. *The lancet*, *395*(10223), 514-523.

Cooper, B. S., Pitman, R. J., Edmunds, W. J. & Gay, N. J. (2006). Delaying the international spread of pandemic influenza. PLoS Med., 3, e212.

Ferguson, N. M., Cummings, D. A., Fraser, C., Cajka, J. C., Cooley, P. C., & Burke, D. S. (2006). Strategies for mitigating an influenza pandemic. *Nature*, *442*(7101), 448-452.

Lemey, P., Rambaut, A., Bedford, T., Faria, N., Bielejec, F., Baele, G., ... & Suchard, M. A. (2014). Unifying viral genetics and human transportation data to predict the global transmission dynamics of human influenza H3N2. PLoS pathogens, 10(2).

Rvachev, L. A., & Longini Jr, I. M. (1985). A mathematical model for the global spread of influenza. Mathematical biosciences, 75(1), 3-22.

Déirdre Hollingsworth, T., Ferguson, N. M. & Anderson, R. M. (2006). Will travel restrictions control the international spread of pandemic influenza. Nat. Med., 12, 497–499.
Hufnagel, L., Brockmann, D., & Geisel, T. (2004). Forecast and control of epidemics in a globalized world. Proceedings of the National Academy of Sciences, 101(42), 15124-15129.
Poletto, C. et al. (2014). Assessment of the Middle East respiratory syndrome coronavirus (MERS-CoV) epidemic in the Middle East and risk of international spread using a novel maximum likelihood analysis approach. Eur. Surveill. 19, 20699.
Skowronski, D. M., Astell, C., Brunham, R. C., Low, D. E., Petric, M., Roper, R. L., ... & Babiuk, L. (2005). Severe acute respiratory syndrome (SARS): a year in review. Annu. Rev. Med., 56, 357-381.
Team, C. S. I., Clarke, T. A., & Park, B. (2003). Preliminary clinical description of severe acute respiratory syndrome. Morbidity and Mortality Weekly Report, 52.
de Wit, E., Rasmussen, A. L., Falzarano, D., Bushmaker, T., Feldmann, F., Brining, D. L., ... & Scott, D. (2013). Middle East respiratory syndrome coronavirus (MERS-CoV) causes transient lower respiratory tract infection in rhesus macaques. Proceedings of the National Academy of Sciences, 110(41), 16598-16603..
Velavan, T. P., & Meyer, C. G. (2020). The Covid-19 epidemic. Tropical medicine & international health: TM & IH.
Yan, G. et al. (2020). Covert COVID-19 and false-positive dengue serology in Singapore. Lancet Infectious Diseases, 2020, 1.
Chapman, W. W., Bridewell, W., Hanbury, P., Cooper, G. F., & Buchanan, B. G. (2001). A simple algorithm for identifying negated findings and diseases in discharge summaries. Journal of biomedical informatics, 34(5), 301-310.
Greenspan, H., Van Ginneken, B., & Summers, R. M. (2016). Guest editorial deep learning in medical imaging: Overview and future promise of an exciting new technique. IEEE Transactions on Medical Imaging, 35(5), 1153-1159.
Shin, H. C., Roth, H. R., Gao, M., Lu, L., Xu, Z., Nogues, I., ... & Summers, R. M. (2016). Deep convolutional neural networks for computer-aided detection: CNN architectures, dataset characteristics and transfer learning. IEEE transactions on medical imaging, 35(5), 1285-1298.
Reprinted from Wang, X., Peng, Y., Lu, L., Lu, Z., Bagheri, M., & Summers, R. M. (2017). Chestx-ray8: Hospital-scale chest x-ray database and benchmarks on weakly-supervised classification and localization of common thorax diseases. Proceedings of the IEEE conference on computer vision and pattern recognition, 2097-2106. Reprint with permission
Xie, S., Girshick, R., Dollár, P., Tu, Z., & He, K. (2017). Aggregated residual transformations for deep neural networks. Proceedings of the IEEE conference on computer vision and pattern recognition, 1492-1500.
Reprinted from Chong, KS. et al. (a) (n.d.). COVID-19 pneumonia. Retrieved March 5, 2020, from https://radiopaedia.org/cases/covid-19-pneumonia-2. Radiopaedia.org, rID: 73893. Reprint with permission
Reprinted from Phan, L. T., Nguyen, T. V., Luong, Q. C., Nguyen, T. V., Nguyen, H. T., Le, H. Q., ... & Pham, Q. D. (2020). Importation and human-to-human transmission of a novel coronavirus in Vietnam. *New England Journal of Medicine, 382*(9), 872-874. Reprint with permission
Reprinted from Liu, Y. C., Liao, C. H., Chang, C. F., Chou, C. C., & Lin, Y. R. (2020). A Locally Transmitted Case of SARS-CoV-2 Infection in Taiwan. New England Journal of Medicine. Reprint with permission
Reprinted from Chen, N., Zhou, M., Dong, X., Qu, J., Gong, F., Han, Y., ... & Yu, T. (2020). Epidemiological and clinical characteristics of 99 cases of 2019 novel coronavirus pneumonia in Wuhan, China: a descriptive study. *The Lancet, 395*(10223), 507-513. Reprint with permission
Reprinted from Silverstein, W. K., Stroud, L., Cleghorn, G. E., & Leis, J. A. (2020). First imported case of 2019 novel coronavirus in Canada, presenting as mild Pneumonia. The Lancet. Reprint with permission

Reprinted from Holshue, M. L., DeBolt, C., Lindquist, S., Lofy, K. H., Wiesman, J., Bruce, H., ... & Diaz, G. (2020). First case of 2019 novel coronavirus in the United States. New England Journal of Medicine. Reprint with permission

Reprinted from Ng, M. Y., Lee, E. Y., Yang, J., Yang, F., Li, X., Wang, H., ... & Hui, C. K. M. (2020). Imaging profile of the COVID-19 infection: radiologic findings and literature review. Radiology: Cardiothoracic Imaging, 2(1), e200034. Reprint with permission

Reprinted from Kong, W., & Agarwal, P. P. (2020). Chest imaging appearance of COVID-19 infection. Radiology: Cardiothoracic Imaging, 2(1), e200028. Reprint with permission

Reprinted from Chong, KS. et al. (b) (n.d.). Hemithorax white-out (Pneumonia) case. Retrieved March 5, 2020, from https://radiopaedia.org/cases/hemithorax-white-out-pneumonia-1?lang=us. Radiopaedia.org, rID: 56908. Reprint with permission

Reprinted from Sheikh, Y. (n.d.). Round pneumonia case. Retrieved March 5, 2020, from https://radiopaedia.org/cases/round-pneumonia-19?lang=us. Radiopaedia.org, rID: 68757 Reprint with permission

Reprinted from Dixon, A. (a) (n.d.). Pneumocystis pneumonia case. Retrieved March 5, 2020, from https://radiopaedia.org/cases/pneumocystis-pneumonia-2?lang=us. Radiopaedia.org, rID: 9613 Reprint with permission

Reprinted from Khateeb, A. (n.d.). Lobar pneumonia case. Retrieved March 5, 2020, from https://radiopaedia.org/cases/lobar-pneumonia?lang=us. Radiopaedia.org, rID: 50499 Reprint with permission

Reprinted from Gaillard, F. (n.d.). Pneumonia case. Retrieved March 5, 2020, from https://radiopaedia.org/cases/pneumonia-7?lang=us. Radiopaedia.org, rID: 11009 Reprint with permission

Reprinted from Alasaly, K., Muller, N., Ostrow, D. N., Champion, P., & FitzGerald, J. M. (1995). Cryptogenic organizing pneumonia. A report of 25 cases and a review of the literature. Medicine, 74(4), 201-211. Reprint with permission

Reprinted from Heyworth, P. (n.d.). Right upper lobe pneumonia case. Retrieved March 5, 2020, from https://radiopaedia.org/cases/right-upper-lobe-pneumonia-9?lang=us. Radiopaedia.org, rID: 60944 Reprint with permission

Reprinted from Knipe, H. (a) (2020). Cavitating pneumonia case. Retrieved March 5, 2020, from https://radiopaedia.org/cases/cavitating-pneumonia-4?lang=us. Radiopaedia.org, rID: 45998 Reprint with permission

Reprinted from Knipe, H. (b) (2020). multilobar pneumonia case. Retrieved March 5, 2020, from https://radiopaedia.org/cases/multilobar-pneumonia?lang=us. Radiopaedia.org, rID: 45998 Reprint with permission

Reprinted from Dixon, A. (b) (n.d.). Right upper lobe pneumonia case. Retrieved March 5, 2020, from https://radiopaedia.org/cases/right-upper-lobe-pneumonia-8?lang=us. Radiopaedia.org, rID: 9613 Reprint with permission